Journal of Structural Geology 30 (2008) 812–817

Contents lists available at ScienceDirect

Journal of Structural Geology

journal homepage: www.elsevier.com/locate/jsg

Implications of simple flexure theory for the formation of saucer-shaped sills

N.R. Goulty [a,*], N. Schofield [b]

[a] Department of Earth Sciences, Durham University, South Road, Durham DH1 3LE, UK
[b] School of Geography, Earth and Environmental Sciences, University of Birmingham, Edgbaston, Birmingham B15 2TT, UK

ARTICLE INFO

Article history:
Received 29 August 2007
Received in revised form 1 April 2008
Accepted 10 April 2008
Available online 23 May 2008

Keywords:
Dolerite
Flexure
Overburden
Plate
Saucer
Sill

ABSTRACT

Saucer-shaped dolerite sills have been identified in several sedimentary basins. They are characteristically sub-circular in plan, with an inner sill connected to a steeply inclined arcuate sheet extending upwards from the edge of the inner sill, and in some cases have raggedly developed flat outer rims. By applying elastic plate theory to the overburden, we obtain an expression for the maximum radius of a circular sill in terms of emplacement depth, excess magma pressure, elastic constants of the overburden and the tensile strain at failure. This expression predicts that the radius of the flat base of a saucer-shaped sill increases with emplacement depth, as observed in the western Karoo Basin, South Africa. Some saucer-shaped sills display an elliptical morphology. From consideration of the flexural strains around the periphery of a horizontal elliptical sill, we infer that saucer-shaped elliptical sills have been fed from below by feeder dykes oriented along the major axis of the ellipse. Flat outer rims would have developed at the final stage of each intrusive episode, when the excess magma pressure was decreasing towards equilibrium with the overburden load. Consequently, flexural strains would also have decreased, so continued intrusion might preferentially occur along a bedding plane.

1. Introduction

Ring-like intrusive structures in the Karoo Basin, South Africa were first described by Du Toit (1920) who interpreted them as being saucer-shaped, flattening out at depth. They are constituents of a very extensive sill complex of Jurassic dolerites intruded into Carboniferous—Permian sediments. Chevallier and Woodford (1999) proposed a mode of emplacement for them involving ring dykes, after reviewing the 20th-century literature on emplacement mechanisms, but concluded that several features remained enigmatic. In recent years many papers have reported observations of sills in offshore basins by seismic reflection imaging. Concave upwards sill complexes, variously described as saucer-shaped, dish-shaped, bowl-shaped and trough-shaped, have been imaged on the NW Australian Shelf (Symonds et al., 1998), offshore Senegal (Rocchi et al., 2007), and along the NE Atlantic margin in the Vøring and Møre basins (Planke et al., 2005; Hansen and Cartwright, 2006), the Faroe-Shetland area (Bell and Butcher, 2002; Smallwood and Maresh, 2002; Hansen et al., 2004) and the Rockall Trough (Thomson, 2004, 2005; Thomson and Hutton, 2004). An example is shown in Fig. 1.

The mechanisms of emplacement of dolerite sill complexes from the walls of feeder dykes have been described by Francis (1982) and Goulty (2005) with reference to the Great Whin and Midland Valley sills in the UK. However, saucer-shaped sills of sub-circular shape in plan have not been identified in either of these sill complexes, which were intruded into faulted basins with a heterogeneous sedimentary infill of limestones and clastic sediments. As was pointed out by Malthe-Sørenssen et al. (2004), saucer-shaped sills have commonly been identified in relatively unstructured basins, where they are generally hosted within clastic sedimentary sequences. Thomson and Hutton (2004) described radially symmetric sill complexes in the North Rockall Trough. Each has a saucer-like inner sill at the base with an arcuate inclined sheet connecting it to a gently inclined, commonly ragged, outer rim. Furthermore, Thomson and Hutton (2004) identified primary, secondary and tertiary flow units branching outwards radially, and hence inferred that each complex had been fed from a source located beneath the centre of the inner sill. The radii of the inner sills in the North Rockall Trough are typically in the range 1 – 3 km, whereas examples in the Karoo studied by Chevallier and Woodford (1999) have radii as great as 20 km. Dips of the inclined arcuate sheets connected to the inner sills for saucer-shaped intrusions in these areas attain values within the range from 20° to 60°.

Here we apply elastic plate theory to the development of circular sills, following Pollard and Johnson (1973) who used the same theory to model the growth of laccoliths. Pollard and Johnson (1973, p. 348) suggest that this simple flexural model is appropriate for circular sills with diameters greater than about 4 times the effective thickness of the overburden; and in an example of its

* Corresponding author.
E-mail address: n.r.goulty@dur.ac.uk (N.R. Goulty).

0191-8141/$ – see front matter © 2008 Elsevier Ltd. All rights reserved.
doi:10.1016/j.jsg.2008.04.002

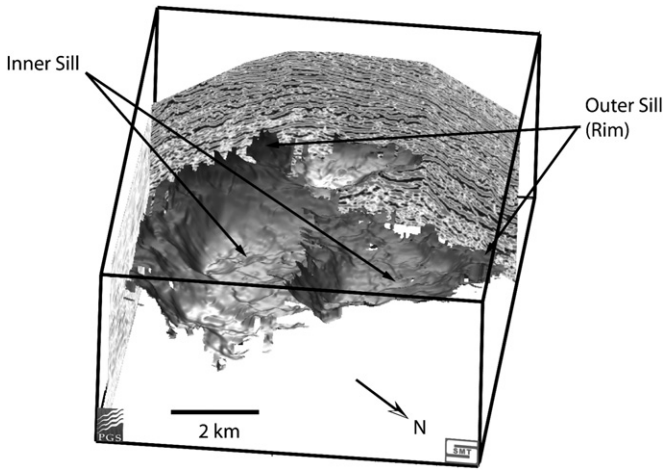

Fig. 1. Set of three saucer-shaped sills in the NE Rockall Trough interpreted from 3-D seismic data, displayed with artificial illumination. The vertical axis is two-way time, over the range 3.0 – 4.0 s from top to bottom of the data cube. The data were supplied by PGS and are displayed using Seismic Micro-Technology's Kingdom software.

application, they showed that the effective thickness may be substantially less than the total thickness. In particular, our aim is to determine the factors which influence the radius of the flat base of the saucer for those saucer-shaped intrusions where there is a relatively abrupt transition between the flat base and the inclined arcuate sheets; we are not attempting to model those saucer-shaped intrusions where the edges of the saucer gradually curve upwards. In this approach, the overburden directly above the sill is treated as a thin elastic plate while the overburden outside the boundary of the sill is assumed to be infinitely rigid and incompressible. Although there are obvious simplifications in this model, there are two points in its favour: it is relatively easy to understand, and it has been successfully applied to a wide variety of geological problems (Watts, 2001; Turcotte and Schubert, 2002). We use it here to model emplacement from a macroscopic viewpoint, without considering the details at the level of individual lobate flow units (Pollard and Johnson, 1973; Thomson and Hutton, 2004).

Two other methods have recently been applied to investigate the mechanics of emplacement of saucer-shaped sills. Malthe-Sørenssen et al. (2004) developed a two-dimensional (2-D) numerical model using a discrete element method in which the host sediments were modelled as a homogeneous elastic material and the magma as a non-viscous fluid. Kavanagh et al. (2006) conducted a series of physical modelling experiments in which dyed water, as a magma analogue, was intruded into solid gelatine, as a crustal analogue. Both approaches have yielded intriguing results, but neither has produced a definitive relationship between the radius of the inner sill (flat saucer base) and other parameters such as emplacement depth, excess magma pressure and sediment properties. We derive such a relationship here, based on the theory of flexure of an elastic plate.

In the following sections, we apply elastic plate theory to the flexure of the overburden above a circular sill and consider the implications regarding the formation of saucer shapes. We then offer two further insights concerning the geometry of saucer-shaped sills, related to the flexural response of the overburden. We infer that the elliptical morphology of some saucer-shaped sills results from them being fed from below by a feeder dyke, and we suggest that flat outer rims developed during the final stages of intrusion when the excess magma pressure had decreased. In the discussion we review the limitations of elastic plate theory in explaining the observed geometry of saucer-shaped sills.

2. Flexure above a circular sill

In applying simple flexure theory to the overburden above a sill, various simplifying assumptions are made (Pollard and Johnson, 1973; Turcotte and Schubert, 2002). The overburden directly above the sill is assumed to be homogeneous and to flex as a thin elastic plate. The boundary conditions applied to the overburden are that the displacements are zero around the periphery, from the edge of the sill to the surface; normal stress equal to the excess magma pressure acts on the base; and the top surface is a free surface (Fig. 2). The sill grows quasi-statically, and the vertical deflection of the overburden is small enough for it to be considered invariant with depth.

For magma to intrude at depth h into sediments of density ρ (Fig. 2), the magma pressure p must be greater than the lithostatic stress due to the weight of the overburden. The excess pressure is

$$\Delta p = p - \rho g h. \tag{1}$$

We adopt cylindrical coordinates with the positive z-axis directed vertically upwards and the r-axis directed radially outwards in the horizontal plane. For a circular sill, the deformation has cylindrical symmetry and so all displacements are independent of azimuth ϕ. The intrusion is centred at $r = 0$ and has radius R. It is convenient to specify the origin of coordinates at elevation $h/2$ above the centre of the sill, where h is the thickness of the overburden, because the horizontal stresses due to the intrusion are zero in the neutral surface at this elevation (Turcotte and Schubert, 2002). The vertical deflection of the plate, w, is the displacement in the positive z-direction, and is assumed to depend only on r.

For small deflections of the plate, the differential equation governing its vertical deflection due to the excess magma pressure is (e.g., Pollard and Johnson 1973)

$$D\nabla^4 w = \Delta p, \tag{2}$$

where the flexural rigidity D is related to Young's modulus E and Poisson's ratio ν by

$$D = \frac{\mathrm{E}h^3}{12(1-\nu^2)}, \tag{3}$$

and ∇^4 is the square of the Laplace operator ∇^2. For a circular sill that grows quasi-statically, imposing the boundary conditions $w = 0$ and $\mathrm{d}w/\mathrm{d}r = 0$ at $r = R$ yields the solution

$$w(r) = \frac{\Delta p}{64D}\left(R^2 - r^2\right)^2, \quad r \le R, \tag{4}$$

for a constant value of the excess magma pressure, Δp (Fig. 3).

The sign convention used here is that extensional strains are positive. The vertical normal strain, $\varepsilon_{zz} = \partial w/\partial z$, due to intrusion of the sill is zero, because w is a function of r only, and the radial normal strain is $\varepsilon_{rr} = \partial u/\partial r$, where u is the displacement in the radial direction and is also a function of r only. By considering the increase in length of the perimeter of a circle of radius r, centred on

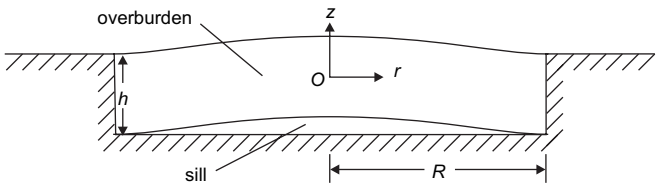

Fig. 2. Schematic vertical section through an intruding circular sill with flexural response of the overburden.

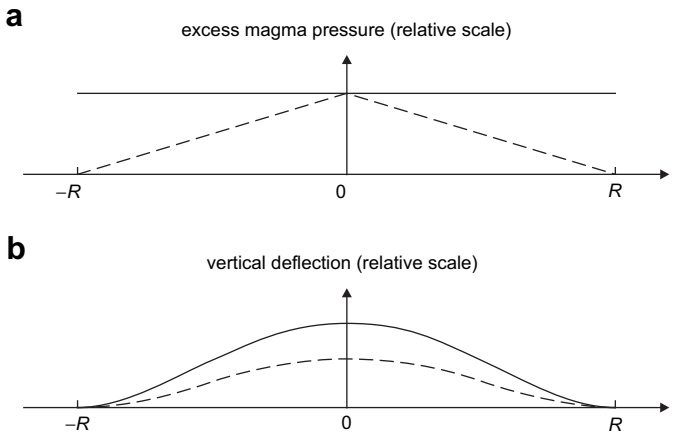

Fig. 3. (a) Excess magma pressure functions acting on the roof of the sill for $r < R$: a constant value Δp (solid line); and a linear decrease from the centre of the sill to zero at the periphery, $\Delta p[1 - r/R]$ (dashed line). (b) Corresponding vertical deflections of the roof of a circular sill: for constant magma pressure (solid line); and linearly decreasing magma pressure (dashed line). As a numerical example to illustrate the amount of vertical deflection that may occur, the solution in Eq. (4) gives a vertical deflection at the centre of the sill, $w(0)$, as 20 m for $\Delta p = 5$ MPa, radius $R = 2000$ m, depth of emplacement $h = 830$ m, Young's modulus $E = 10^3$ MPa, and Poisson's ratio $\nu = 0.48$. These last two values for the elastic constants are appropriate for soft clastic sediment.

the z-axis, when undergoing a small radial displacement u, it may be seen that the tangential normal strain is

$$\varepsilon_{\phi\phi} = \frac{u}{r}. \tag{5}$$

For elastic flexure of a thin bed,

$$\frac{\partial u}{\partial r} = -z\frac{\mathrm{d}^2 w}{\mathrm{d}r^2} \tag{6}$$

everywhere above the sill, with $z = 0$ at the neutral surface at height $h/2$ above the sill (Turcotte and Schubert, 2002). Using Eqs. (3), (4) and (6), the radial strain at the roof of the sill is

$$\frac{\partial u}{\partial r} = \frac{3(1-\nu^2)\,\Delta p}{8Eh^2}\left(3r^2 - R^2\right), \quad z = -h/2, \quad r < R. \tag{7}$$

The radial strain in the roof increases with r, and towards the boundary of the sill becomes

$$\frac{\partial u}{\partial r} = \frac{3(1-\nu^2)\,\Delta p R^2}{4Eh^2}, \quad z = -h/2, \quad r \to R. \tag{8}$$

For the same numerical example as that given in the caption to Fig. 3, the tensile radial strain in the roof at the periphery of the sill is 1.7×10^{-2}. This maximum tensile radial strain increases with the square of the sill radius, so when the sill has grown sufficiently in the horizontal plane, tensile failure will occur in the roof at its boundary. It is this point which provides the justification for our application of simple flexure theory to the intrusion of concentric sills. Although the theory is simplistic, as explained in the discussion section below, it does predict that circular sills cannot grow indefinitely in size in the horizontal plane without tensile failure in the roof.

For completeness, we evaluate the other components of the strain tensor in the roof of the sill. Integrating Eq. (6),

$$u = -z\frac{\mathrm{d}w}{\mathrm{d}r} \tag{9}$$

above the sill. The constant of integration is zero because $u = 0$ and $\mathrm{d}w/\mathrm{d}r = 0$ at $r = 0$. This equation justifies the imposition of the second boundary condition used to obtain the solution in Eq. (4): the assumption that there is no displacement around the edge of the circular plate means that $u = 0$ at $r = R$, so it follows from Eq. (9) that $\mathrm{d}w/\mathrm{d}r = 0$ at $r = R$. It also follows from Eq. (9) that

$$\frac{\partial u}{\partial z} = -\frac{\mathrm{d}w}{\mathrm{d}r}, \tag{10}$$

so the shear component of the strain tensor, $\varepsilon_{rz} = (\partial w/\partial r + \partial u/\partial z)/2$, due to the intrusion is zero everywhere above the sill. In fact, there must be shear stress acting downwards along any cylindrical surface of constant r in the overburden, where $r < R$, to balance the upward force due to excess magma pressure acting on the base of the cylinder, but the distortions due to this shear stress are negligible compared with those related to the bending moment (Pollard and Johnson, 1973). By symmetry, the other shear components of the strain tensor, $\varepsilon_{\phi z}$ and $\varepsilon_{r\phi}$, are also zero, so ε_{rr}, $\varepsilon_{\phi\phi}$ and ε_{zz} are principal strains; but ε_{zz} is zero too, so the overburden is in a state of plane strain.

Substitution of Eq. (4) into Eq. (9) yields

$$u = \frac{\Delta p}{16D}\left(R^2 - r^2\right)rz. \tag{11}$$

From Eqs. (5) and (11) it may be seen that the tangential principal strain $\varepsilon_{\phi\phi}$ is compressional in the roof of the sill, where $z = -h/2$, and reaches a maximum value of zero as $r \to R$. Thus the maximum tensile strain in the roof of the sill is indeed the radial principal strain at its boundary.

In the above analysis, we have assumed a constant value for the excess magma pressure. However, thanks to the homogeneous nature of Eq. (2), it is straightforward to find solutions for any excess magma pressure distribution which is a polynomial function of the radial coordinate, r. For example, if the excess magma pressure decreases linearly from Δp at the centre of the sill to zero at the periphery, Eq. (2) is replaced by

$$D\nabla^4 w = \Delta p[1 - r/R], \tag{12}$$

and for the same boundary conditions the solution is

$$w(r) = \frac{\Delta p}{14400D}\left(129R^4 - 290R^2r^2 + 225r^4 - 64r^5/R\right), \quad r \le R. \tag{13}$$

In this case, the tensile strain is again a maximum in the radial direction at the periphery of the sill, and the form of the vertical deflection of the overburden is remarkably similar to the solution for a constant value of excess magma pressure (Fig. 3).

3. Predicted size of the inner sill

The flexural analysis given in the preceding section has predictive value for the relationship between the radius of the flat base of a saucer-shaped sill, the depth of intrusion and the excess magma pressure. Eq. (8) shows that for a circular sill of radius R the radial strain is at its maximum value as $r \to R$, so tensile failure of the roof is expected to occur preferentially at the edge of the sill. We can rearrange this equation to find the radius that the circular sill has attained when tensile failure takes place in its roof. It is given by

$$R = 2h\sqrt{\frac{E\varepsilon_f}{3(1-\nu^2)\,\Delta p}}, \tag{14}$$

where ε_f is the value of radial tensile strain at failure. Malthe-Sørenssen et al. (2004) have suggested that tensile strains at failure in the host sediments may lie in the range 2×10^{-3} to 2×10^{-2}.

With uniform lithology and a constant value of excess magma pressure, Eq. (14) implies that the radius of the sill when tensile failure occurs in its roof would be proportional to the depth of intrusion, h. In reality, the elastic moduli and the tensile radial strain at failure may vary with depth, and the excess magma pressure may vary with both time and depth. Even so, we may reasonably suppose that at some level of approximation for a single regional intrusive episode, the radius of the circular inner sill is related to the emplacement depth by a power law function of the form

$$R = ah^b, \tag{15}$$

where a and b are positive constants. Thus the application of simple flexure theory to the mechanics of intrusion of saucer-shaped sills could be tested against observations in 3-D seismic datasets. Suitable datasets would need to image a sufficient number of sills for which the radius of the flat base and emplacement depth could be estimated. In this context, it is interesting to note the following remark by Chevallier and Woodford (1999) concerning "the extensive coalescing circular units" in the western Karoo dolerite sills: "The size of the ring complex appears to be related to the stratigraphic level of intrusion, that is, the sills forming the larger structures have been intruded at the base of the Karoo sequence, while the smaller structures (<10 km diameter) have been intruded into the upper part of the sequence." Eqs. (14) and (15) are in accord with this observation.

There are alternative uses for Eq. (14). For uniform overburden lithology, it predicts that the excess magma pressure Δp is proportional to h^2/R^2. A necessary condition for eruption is that the magma pressure p is greater than the hydrostatic pressure due to a column of magma reaching the surface, $\rho_m g h$, where ρ_m is the magma density. Substitution of Eqs. (1) and (12) into this condition, with elimination of p and Δp, yields

$$\frac{h}{R^2} > \frac{3(1-\nu^2)(\rho_m - \rho)g}{4E\varepsilon_f} \tag{16}$$

as the necessary condition for magma eruption. Hence, the greater the function h/R^2, the more likely it is that there will have been eruption. This prediction could help in determining whether structures seen above sub-circular sills in 3-D seismic data represent forced folds or volcanic edifices (e.g., Hansen and Cartwright 2006, 2007; Thomson, 2007). From variations in the value of h/R^2 between saucers intruded in the same episode, relative values of excess magma pressure could be inferred and correlated with cross-cutting relationships or precise dating to estimate changes in magma head over time.

4. Elliptical saucer-shaped sills

The incremental strain and stress tensors in the overburden above an intruding circular sill have cylindrical symmetry, with horizontal principal axes in the radial and tangential directions. However, several saucer-shaped sills in the western Karoo are elliptical in plan, as are some that have been imaged elsewhere on 3-D seismic data (Thomson and Hutton, 2004). The Golden Valley Sill, near Queenstown, South Africa, is a spectacular outcrop example of an elliptical saucer-shaped dolerite intrusion (Fig. 4). In this section, we propose and justify a simple hypothesis to explain the elliptical shapes. The hypothesis is that an elliptical saucer-shaped sill has been fed from below by a feeder dyke oriented along the major axis of the ellipse.

We suppose that a planar sill, intruded along a bedding plane and fed by a dyke from below, is typically elongated along the direction of dyke strike in an approximately elliptical shape. The question we need to answer is whether tensile failure would first occur in the roof of the sill at its periphery along the major axis, or along the minor axis. Let such an elliptical sill occupy the area $x^2/a^2 + y^2/b^2 \le 1$ in the horizontal plane, where the major axis of the ellipse is the x-axis (i.e., $a > b$). Pollard and Johnson (1973) quoted the solution to Eq. (2) for the boundary conditions $w = \partial w/\partial x = \partial w/\partial y = 0$ at $x^2/a^2 + y^2/b^2 = 1$ with constant excess magma pressure, Δp, as

$$w = \frac{\Delta p}{8D}\left(1 - \frac{x^2}{a^2} - \frac{y^2}{b^2}\right)^2 \Big/ \left(\frac{3}{a^4} + \frac{3}{b^4} + \frac{2}{a^2 b^2}\right) \tag{17}$$

By using equations equivalent to Eq. (6), it is easy to show that the tensile strains in the roof of the sill, approaching its periphery, along the minor axis are greater than those along the major axis by the factor $(a/b)^2$. Consequently, as a planar sill that is initially elliptical expands, it is to be expected that tensile failure of the roof would occur first at the two points where the minor axis of the ellipse reaches the periphery. Thus a sill which initially intrudes the bedding with an elliptical shape has no tendency to become more concentric when it develops into a saucer shape: on the contrary,

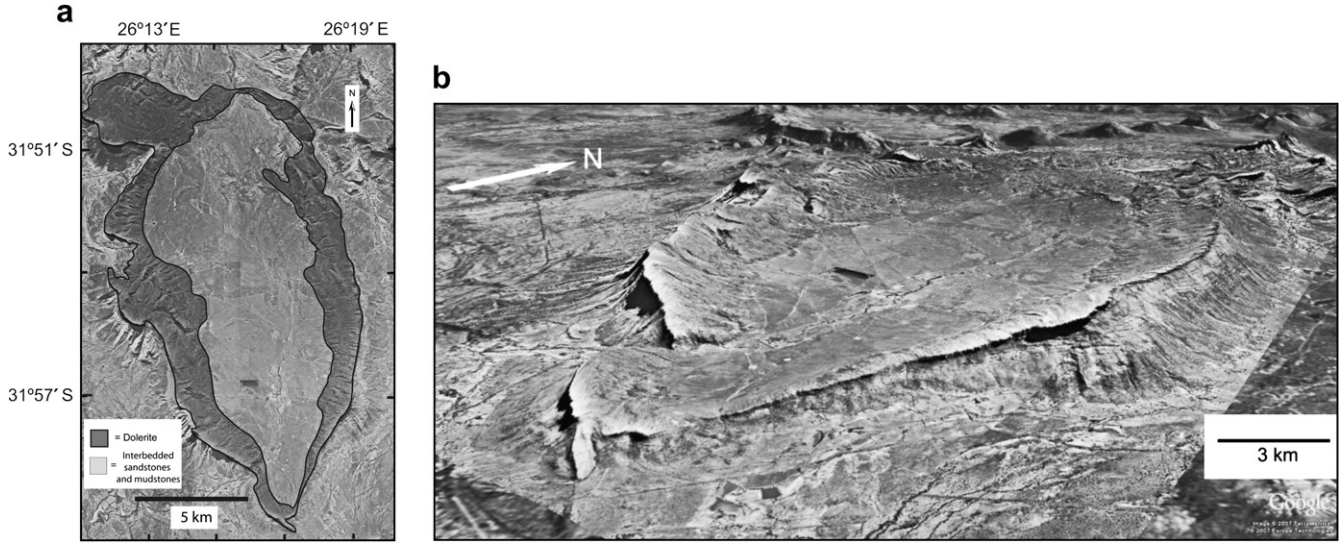

Fig. 4. The Golden Valley Sill: (a) map view from aerial photographs with geological interpretation overlaid; (b) oblique view from the Google Earth™ mapping service.

the eccentricity of the elliptical shape is likely to be enhanced. Furthermore, if the inclined fractures at the edge of the sill grow outwards around the periphery of the sill from the minor axis, as well as propagating upwards, the initial elliptical shape of the planar sill would develop into a more eye-shaped morphology. Arguably, the Golden Valley Sill developed in this way because it appears more eye-shaped than elliptical in plan view (Fig. 4a).

The corollary to this simple hypothesis for elliptical saucer-shaped sills is that circular saucer-shaped sills are likely to have been fed from a central point, which might either be a pipe-like feeder or a single lobate protrusion from an underlying saucer-shaped sill (Cartwright and Hansen, 2006).

5. Flat outer rims

Some of the saucer-shaped dolerite sills in the Karoo Basin have flat outer rims, as described by Chevallier and Woodford (1999). Due to erosion, it is not possible to be certain whether these flat outer rims formed around the complete circumference of the inner sills in the Karoo. Thomson and Hutton (2004) described the outer rims of saucer-shaped sills in the North Rockall Trough as "commonly ragged", and several saucer-shaped sills have been imaged on 3-D seismic data without any identified outer rim. The result of a 2-D numerical modelling experiment reported by Malthe-Sørenssen et al. (2004) had a flat inner sill connected to upward propagating steeply inclined sheets at either side which were, at their upper edges, connected to more gently dipping outer sheets. However, there was insufficient evaluation of that result to draw any clear conclusion about it.

We note that particular bedding planes in the host sediments are likely to be predisposed towards intrusion by sills because they have low tensile strength. We further suggest that a key factor in the development of outer rims is a reduction in excess magma pressure because outer rims developed during the final stage of intrusion. As the excess magma pressure decreases, flexural strains in the overburden must decrease, but intrusion continues until the magma pressure has fallen far enough for equilibrium to be established between the magma pressure and the weight of the overburden. With reduced flexural strains, intrusion preferentially occurs along bedding planes due to the low tensile strength normal to these surfaces, as generally occurs during the early stages of sill intrusion.

6. Discussion

According to the simple flexure theory given above, the principal strains due to the intrusion at the edge of the sill are zero in the vertical and tangential directions, whilst the radial tensile strain has its maximum value approaching the edge. Such a strain response would imply that the tensile fracture at the boundary of the flat base of the sill should initially propagate vertically upwards. It is of interest to note that Pollard and Johnson (1973, Fig. 16) found that tensile fractures did develop perpendicular to the roof of the sill in physical modelling experiments, when grease was injected into horizontal cracks between gelatine layers, or between plexiglass and overlying semi-brittle layers.

However, there are no reported observations from fieldwork or 3-D seismic interpretation which confirm that tensile failure of the roof initiates as a vertical crack. We affirm that the simple flexure theory adopted here for the overburden above a planar intrusion is only a partial model for the process of intrusion. It is applicable up to the point when tensile failure takes place in the roof of the sill, but makes no predictions about the subsequent propagation direction of the rupture.

A related weakness in the flexural model is that there is a discontinuity in the radial strain within the overburden at $r = R$. This discontinuity results from the assumed boundary condition that displacements are zero at all points around the edge of the plate, on the cylindrical surface which extends vertically upwards from the periphery of the sill to the surface. In effect, this boundary condition is equivalent to introducing an abrupt change in material parameters in the model, with the overburden above the level of intrusion being assumed to be incompressible and infinitely rigid where $r > R$. In spite of these gross assumptions, we contend that the flexural model is useful because it provides a partial explanation for the saucer shapes and predicts a testable relationship between the radius of the flat base of a saucer-shaped sill and other parameters.

7. Conclusions

The theory of flexure for an elastic plate has been applied to the deformation of the overburden above a growing circular sill. According to the theory, the intrusion causes tensile strain in the immediate roof of the sill only in the radial direction, with its maximum value at the boundary of the sill. The value of maximum tensile strain increases with sill radius, and so we may suppose that when the circular sill has grown sufficiently, this tensile strain reaches the tensile strain for failure of the overburden. Consequently, steeply inclined arcuate sheets may be expected to develop around the periphery of circular sills to generate saucer-shaped intrusions.

Our main result is encapsulated in Eq. (14) which expresses the radius of the flat inner sill in terms of emplacement depth, excess magma pressure, elastic constants of the overburden and the tensile strain at failure. The relationship predicts an increase in radius of the inner sill with increasing emplacement depth, as observed in the western Karoo (Chevallier and Woodford, 1999). Two further insights reported here are explanations for the elliptical morphology of some saucer-shaped sills and the development of flat outer rims in some cases. Consideration of the flexural strains due to an elliptical intrusion from an underlying feeder dyke located along the major axis of the ellipse suggests that tensile failure will occur first at points where the minor axis of the ellipse reach the periphery. Development of flat outer rims occurs during the final stages of sill intrusion, when the excess magma pressure is falling and flexural strains are reduced so that intrusion preferentially occurs along a bedding plane.

Acknowledgements

NS is grateful to the late Ken Thomson for inspirational supervision in this subject area, and to NERC for providing his research studentship (NER/S/A/2005/13237). We thank Carl Stevenson and Graham Westbrook for discussions, Thierry Menand and Sven Morgan for very constructive reviews, and Tom Blenkinsop for editorial guidance.

References

Bell, B., Butcher, H., 2002. On the emplacement of sill complexes: evidence from the Faroe-Shetland Basin. In: Jolley, D.W., Bell, B.R. (Eds.), The North Atlantic Igneous Province: Stratigraphy, Tectonic, Volcanic ands Magmatic Processes. Special Publication, vol. 197. Geological Society, London, pp. 307–329.

Cartwright, J., Hansen, D.M., 2006. Magma transport through the crust via interconnected sill complexes. Geology 34, 929–932.

Chevallier, L., Woodford, A., 1999. Morpho-tectonics and mechanism of emplacement of dolerite rings and sills of the western Karroo, South Africa. South African Journal of Geology 102, 43–54.

Du Toit, A.L., 1920. The Karoo dolerites of South Africa: a study in hypabyssal injection. Transactions of the Geological Society of South Africa 23, 1–42.

Francis, E.H., 1982. Magma and sediment—I: emplacement mechanism of late Carboniferous tholeiite sills in northern Britain. Journal of the Geological Society, London 139. 1-20.

Goulty, N.R., 2005. Emplacement mechanism of the Great Whin and Midland Valley dolerite sills. Journal of the Geological Society, London 162. 1047-1056.

Hansen, D.M., Cartwright, J., 2006. The three-dimensional geometry and growth of forced folds above saucer-shaped igneous sills. Journal of Structural Geology 28, 1520–1535.

Hansen, D.M., Cartwright, J., 2007. Reply to comment by K. Thomson on "The three-dimensional geometry and growth of forced folds above saucer-shaped sills" by D.M. Hansen and J. Cartwright. Journal of Structural Geology 29, 741–744.

Hansen, D.M., Cartwright, J.A., Thomas, D., 2004. 3D seismic analysis of igneous sill complexes and the geometry of sill junctions. In: Davies, R.J., Cartwright, J.A., Stewart, S.A., Lappin, M., Underhill, J.R. (Eds.), 3D Seismic Technology: Application to the Exploration of Sedimentary Basins. Memoir, vol. 29. Geological Society, London, pp. 199–208.

Kavanagh, J.L., Menand, T., Sparks, R.S.J., 2006. An experimental investigation of sill formation and propagation in layered elastic media. Earth and Planetary Science Letters 245, 799–813.

Malthe-Sørenssen, A., Planke, S., Svensen, H., Jamtveit, B., 2004. Formation of saucer-shaped sills. In: Breitkreuz, C., Petford, N. (Eds.), Physical Geology of High-Level Magmatic Systems. Special Publication, vol. 234. Geological Society, London, pp. 215–227.

Planke, S., Rasmussen, T., Rey, S.S., Myklebust, R., 2005. Seismic characteristics and distribution of volcanic intrusions and hydrothermal vent complexes in the Vøring and Møre basins. In: Doré, A.G., Vining, B. (Eds.), Petroleum Geology: North-West Europe and Global Perspectives – Proceedings of the 6th Petroleum Geology Conference. Geological Society, London, pp. 833–844.

Pollard, D.D., Johnson, A.M., 1973. Mechanics of growth of some laccolithic intrusions in the Henry Mountains, Utah, II: bending and failure of overburden layers and sill formation. Tectonophysics 18, 311–354.

Rocchi, S., Mazzotti, A., Marroni, M., Pandolfi, L., Costantini, P., Giuseppe, B., di Biase, D., Federici, F., Goumbo Lô, P., 2007. Detection of Miocene saucer-shaped sills (offshore Senegal) via integrated interpretation of seismic, magnetic and gravity data. Terra Nova 19, 232–239.

Smallwood, J.R., Maresh, J., 2002. The properties, morphology and distribution of igneous sills: modelling, borehole data and 3D seismic from the Faroe—Shetland area. In: Jolley, D.W., Bell, B.R. (Eds.), The North Atlantic Igneous Province: Stratigraphy, Tectonic, Volcanic ands Magmatic Processes. Special Publication, vol. 197. Geological Society, London, pp. 271–306.

Symonds, P.A., Planke, S., Frey, Ø., Skogseid, J., 1998. Volcanic development of the Western Australian continental margin and its implications for basin development. In: Purcell, P.G., Purcell, R.R. (Eds.), The Sedimentary Basins of Western Australia 2, Proceedings of the Petroleum Exploration Society of AustraliaSymposium, Oxford. Petroleum Exploration Society of Australia, Perth, pp. 33–54.

Thomson, K., 2004. Sill complex geometry and internal architecture: a 3D seismic perspective. In: Breitkreuz, C., Petford, N. (Eds.), Physical Geology of High-Level Magmatic Systems. Special Publication, vol. 234. Geological Society, London, pp. 229–232.

Thomson, K., 2005. Extrusive and intrusive magmatism in the North Rockall Trough. In: Doré, A.G., Vining, B. (Eds.), Petroleum Geology: North-West Europe and Global Perspectives – Proceedings of the 6th Petroleum Geology Conference. Geological Society, London, pp. 1620–1631.

Thomson, K., 2007. Comment on "The three-dimensional geometry and growth of forced folds above saucer-shaped igneous sills" by Hansen and Cartwright. Journal of Structural Geology 29, 736–740.

Thomson, K., Hutton, D., 2004. Geometry and growth of sill complexes: insights using 3D seismic data from the North Rockall Trough. Bulletin of Volcanology 66, 364–375.

Turcotte, D.L., Schubert, G., 2002. Geodynamics. Cambridge University Press.

Watts, A.B., 2001. Isostasy and Flexure of the Lithosphere. Cambridge University Press.